JMEPEG (2006) 15:130-138
DOI: 10.1361/105994906X83411

1059-9495/$19.00

Performance of High-Velocity Oxyfuel-Sprayed Coatings on an Fe-Based Superalloy in Na_2SO_4-60%V_2O_5 Environment at 900 °C Part II: Hot Corrosion Behavior of the Coatings

T.S. Sidhu, S. Prakash, and R.D. Agrawal

(Submitted May 25, 2005: in revised form August 9, 2005)

NiCrBSi, Cr_3C_2-NiCr, Ni-20Cr, and Stellite-6 coatings were deposited on an Fe-based superalloy by the high-velocity oxyfuel (HVOF) thermal spray process. The hot corrosion behavior of the coatings in an aggressive environment of Na_2SO_4-60%V_2O_5 at 900 °C under cyclic conditions was studied. The thermogravimetric technique was used to establish the kinetics of corrosion. X-ray diffraction, scanning electron microscopy/energy-dispersive x-ray and electron probe microanalysis techniques were used to analyze the corrosion products. Hot corrosion resistances of all the coatings were found to be better than the uncoated superalloy. The Ni-20Cr coating was found to be the most protective, followed by Cr_3C_2-NiCr coatings. The Ni-20Cr coating had reduced the mass gain by 90% of that gained by the uncoated superalloy. The hot corrosion resistance shown by the Cr_3C_2-NiCr coating was slightly better compared with the NiCrBSi coating; however, both of the coatings performed better than the Stellite-6 coating. The Stellite-6 coating was the least effective among the coatings studied, but it was still successful in decreasing the mass gain to about one fourth compared with the uncoated superalloy. The formation of oxides and spinels of nickel, chromium, or cobalt may be contributing to the development of hot corrosion resistance in the coatings. This article focuses on the hot corrosion behavior of HVOF coatings. The characterization of these coatings has been presented in part I included in this issue.

Keywords high-velocity oxyfuel spray coatings, hot corrosion, protective coatings, superalloy

1. Introduction

Hot corrosion is an accelerated form of oxidation that occurs when metals and alloys are heated to the temperature range of 700 to 900 °C, in the presence of sulfate deposits formed as a result of the reaction between sodium chloride and sulfur compounds in the gas phase surrounding the metal (Ref 1, 2). At higher temperatures, the deposits of Na_2SO_4 are molten (melting point 884 °C) and can cause accelerated corrosion. The accelerated corrosion can also be caused by other salts, such as vanadates or sulfate-vanadate mixtures, and in the presence of solid or gaseous salts such as chlorides (Ref 3).

Advances in materials development and cooling schemes will lead to increases in the operation temperatures of gas turbines, boilers, and industrial waste incinerators. The combination of such high temperatures with environmental contaminants and low-grade fuels, such as sodium, sulfur, vanadium, and chlorine, require special attention to the phenomenon of hot corrosion. This form of corrosion, unlike oxidation, can consume the material at an unpredictably rapid rate. Consequently, the load-carrying ability of the components is reduced, leading eventually to its catastrophic failure (Ref 4). The inability either to totally prevent the hot corrosion or at least to detect it at an early stage has resulted in several accidents, leading to loss of life and/or the destruction of engines/infrastructures.

No alloy is immune to hot corrosion attack indefinitely. The presence of combustion gases constitutes an extreme environment, and hot corrosion is inevitable when the alloys are used at high temperatures for longer periods of time. Superalloys are designed for high-temperature applications, but they are not able to meet the parameters of both high-temperature strength and high-temperature corrosion resistance simultaneously (Ref 5, 6). So, the superalloys need to be protected, but the protection system must be practical, reliable, and economically viable.

Coatings enhance the life of the materials by protecting them against wear or corrosion (Ref 7). Currently, diffusion and overlay coatings are used to provide corrosion and oxidation resistance to extend the component life (Ref 8). However, as the operating temperatures of the gas turbines have increased, it has become impossible to achieve the required service lives using diffusion coatings, whereas overlay coatings have performed better in aggressive environments at elevated temperatures (Ref 9).

In recent years, there has been a growing interest in the use of high-velocity oxyfuel (HVOF) processes to deposit protective overlay coatings onto the surfaces of engineering components to allow them to function under extreme conditions of wear, erosion-corrosion, high-temperature oxidation, and hot corrosion. The HVOF coatings have high hardness and good

T.S. Sidhu, S. Prakash, and **R.D. Agrawal,** Metallurgical & Materials Engineering Department, Indian Institute of Technology Roorkee, Roorkee-247 667, India. Contact e-mail: tssidhu@rediffmail.com.

adhesion values with a porosity of less than 1%, and have been widely adopted in many industries due to their flexibility and cost-effectiveness (Ref 10, 11). Therefore, in this study, the HVOF process has been selected to deposit the coatings for the evaluation of their hot corrosion behavior.

The purpose of a coating is to serve as an effective solid-state diffusion barrier between oxygen (or other gases) and the base alloy. The coating should have a composition that will react with the environment to produce the protective oxide scale, which should not react with the corrosive environment and at the same time should not allow the corrosive species to diffuse into the coating. Therefore, the identification/development of suitable alloys and coatings are of great interest for such applications (Ref 12-14).

The Ni-base coatings are used in applications in which wear resistance combined with oxidation or hot corrosion resistance is required. Nickel-base self-fluxing alloys are currently used in the chemical industry, petroleum industry, glass mould industry, hot working punches, and fan blades, and for mud-purging elements in cement factories (Ref 15-20). NiCrBSi coatings are used in high-temperature applications. The addition of chromium promotes oxidation and corrosion resistance at elevated temperatures, and increases the hardness of the coating by the formation of hard phases. Boron depresses the melting temperature and contributes to the formation of hard phases. Silicon is added to increase the self-fluxing properties (Ref 21, 22).

The high resistance of high-chromium, nickel-chromium alloys to high-temperature oxidation and corrosion allows them to be widely used as welded and thermally sprayed coatings in fossil fuel-fired boilers, waste incineration boilers, and electric furnaces (Ref 23, 24). The HVOF process is often used to deposit high-chromium, nickel-chromium coatings onto the outer surfaces of various parts of boilers (e.g., tubes) to prevent the penetration of hot gases, molten ash, and liquids to less noble carbon steel boiler tubes.

A cobalt-based alloy containing chromium, tungsten, and carbon, which is known as Stellite-6, has high hardness at high temperature, high corrosion resistance, and wear resistance (Ref 25, 26). However, there have not been much reporting on the hot corrosion behavior of Stellite-6 (Ref 27).

Sulfur, sodium, and vanadium are common impurities in the low-grade petroleum fuels. Molten sulfate-vanadate deposits resulting from the condensation of combustion products of such fuels are extremely corrosive to high-temperature materials in the combustion systems. Further, the mixture of Na_2SO_4 and V_2O_5 in a ratio of 40:60 constitutes the eutectic with a low melting point of 550 °C and provides a very aggressive environment for hot corrosion to occur (Ref 28). A cyclic study of 50 cycles (cycle of 1 h of heating and 20 min of cooling) is considered to be adequate for the steady-state oxidation of the material (Ref 29-31). The cyclic study provides the most severe conditions for testing and represents the actual industrial environment where breakdown and shutdown frequently occur. Metal corrosion problems in actual applications are more or less cyclic rather than isothermal (Ref 32). Cyclic study of the candidate HVOF coatings in the given molten salt environment is not available in the open literature.

So, the objective of this study is to evaluate the hot corrosion behavior of HVOF-sprayed coatings of NiCrBSi, Cr_3C_2-NiCr, Ni-20Cr, and Stellite-6 on an Fe-based superalloy, namely Superfer 800H (similar grade Incoloy 800H) in an aggressive environment of molten salt Na_2SO_4-60%V_2O_5 at 900 °C under cyclic conditions. The substrate superalloy has been provided by Mishra Dhatu Nigam Limited (Hyderabad, India) to find suitable protective coatings for extending the life of the superalloy at the upper end of its performance capabilities in hot corrosion conditions.

X-ray diffraction (XRD), optical microscope, scanning electron microscopy (SEM)/energy-dispersive x-ray (EDAX) analysis, and electron probe microanalysis (EPMA) techniques have been used to analyze the corrosion products after hot corrosion at 900 °C.

2. Experimental Procedure

2.1 Development and Characterization of the Coatings

The Fe-based superalloy Superfer 800H, developed by M/S Mishra Dhatu Nigham Limited, was used as a substrate material. Four types of commercially available coating alloys (Cr_3C_2-NiCr, NiCrBSi, and Stellite-6 in the powder form, and Ni-20Cr in the wire form) were used in the study. Details of the composition of the substrate, and the coating alloys and characterization of the coatings have been specified in sections 2.1 and 2.2 of part I.

2.2 Molten Salt Corrosion Tests

Cyclic studies were performed in molten salt (Na_2SO_4-60%V_2O_5) for 50 cycles. Each cycle consisted of 1 h of heating at 900 °C in a silicon carbide tube furnace followed by 20 min of cooling at room temperature. The cyclic study provides the most severe conditions for testing and represents the actual industrial environment, where breakdown and shutdown occur frequently. A cyclic study of 50 cycles had been performed as the study of 50 cycles (a cycle consisted of 1 h of heating and 20 min of cooling) is considered to be adequate for the steady-state oxidation of the material (Ref 29-31). The studies were performed for uncoated as well as coated specimens for the purpose of comparison. The specimens were mirror polished down to 1 μm alumina wheel cloth polishing before the corrosion run. A coating of uniform thickness with 3 to 5 mg/cm^2 Na_2SO_4-60%V_2O_5 was applied with a camel hairbrush on the preheated sample (250 °C). The mass change measurements were taken at the end of each cycle with the help of an Electronic Balance machine (model 06120, Contech, India) with a sensitivity of 1 mg. The spalled scale was also included at the time of measuring mass change at the end of each cycle to determine the total rate of corrosion. Efforts were made to formulate the kinetics of corrosion. X-ray diffraction, SEM/EDAX, and EPMA techniques were used to analyze the corrosion products after hot corrosion. The details of these instruments are given in section 2.2 of part I.

3. Results

3.1 Corrosion Kinetics in Molten Salt

The mass gain plots for the substrate superalloy for 50 cycles with and without coatings, in the presence of a salt layer of Na_2SO_4-60%V_2O_5 at 900 °C, have been shown in Fig. 1. The uncoated superalloy has shown a nearly parabolic behavior and a maximum mass gain. The coated superalloy in all four cases has shown a much lower mass gain compared with the uncoated superalloy in the given molten salt environment. The

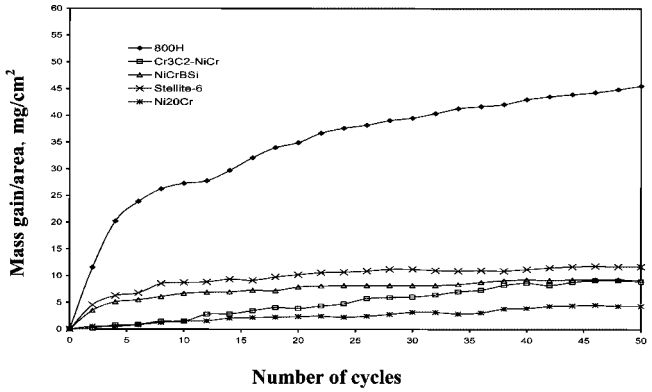

Fig. 1 Mass gain versus the number of cycles plot for coated and uncoated superalloy 800H that has been subjected to cyclic oxidation for 50 cycles in Na_2SO_4-60%V_2O_5 at 900 °C

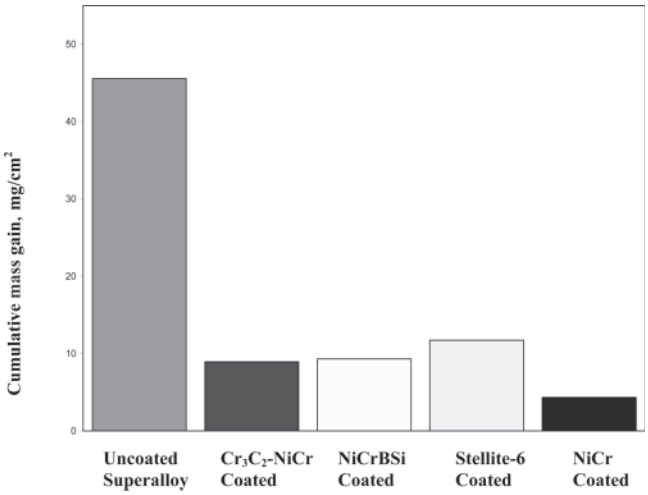

Fig. 2 Bar chart showing cumulative mass gain per unit area for coated and uncoated superalloy 800H that has been subjected to cyclic oxidation for 50 cycles in Na_2SO_4-60%V_2O_5 at 900 °C

Ni-20Cr wire-coated superalloy has shown a minimum mass gain that is approximately one eleventh of that gained by the uncoated superalloy. The Cr_3C_2-NiCr-coated superalloy has shown a second minimum mass gain that is less than one fifth of that indicated by uncoated superalloys, whereas the mass gain by the NiCrBSi-coated superalloy is a little more than one fifth and the Stellite-6 coated is less than one fourth of that shown by the bare superalloy. The Stellite-6-coated superalloy has shown a maximum mass gain compared with other coated superalloys; still, its mass gain is less than one fourth that of the uncoated superalloy. Figure 2 shows the cumulative mass gain/unit area in all the five cases.

During the study, it was observed that the bare superalloy underwent intense spalling as well as sputtering (disintegration of the scale accompanied by cracking sound during cooling). Spalling of the superalloy was started from the third cycle onward, which intensified as the period of study progressed with a lot of corrosion products seen in the boat. Sputtering of the corrosion products was also spotted during the 8th cycle, and heavy sputtering was observed after the 10th cycle onward. Sputtering continued while the sample was getting cooled at the end of each cycle or keeping the boat inside the furnace, which had affected the mass gained by the bare superalloy, and the actual mass gain might be more than what was observed. The surface of the specimen, which turned a shining black color during the second cycle, became rough as the study progressed, and a uniform pitting was observed on the surface.

The Cr_3C_2-NiCr coatings had shown some minor cracks at the edges and corners, and spalling from these regions had been observed. Scale with a blackish green color was formed on the Cr_3C_2-NiCr-coated superalloy, and minor spallation of the scale become apparent after the 15th cycle onward. However, after the 31st cycle, further spallation of the scale was not observed, but the coating had broken from one corner of the specimen during the last cycle (Fig. 3b). A compact and dense continuous scale of a rust color, with some voids, was observed to form on the NiCrBSi-coated superalloys and no spallation or peeling from the scale was noticed even at the corners or edges (Fig. 3c, 5c). Wang et al. (Ref 33) reported that the addition of Si and B can promote the formation of continuous and dense scale in the initial corrosion stage, and can improve the adherence of the outer scale to the coating in the subsequent hot corrosion process. So, the behavior of this coating was in good agreement with the findings of Wang et al. (Ref 33), and no spalling or peeling of the scale was observed. However, some voids in the scale were noticed at the end of 50 cycles. Ni-20Cr coatings had shown negligible spallation behavior that too is confined to the corners and edges. Scale with a shining gray color was formed, and green-colored spots were observed where spallation of scale took place (Fig. 3e). The Stellite-6 coating had shown spalling and peeling behavior from the 6th cycle onward in the form of blackish powdered particles. After the 17th cycle, no further spallation was observed.

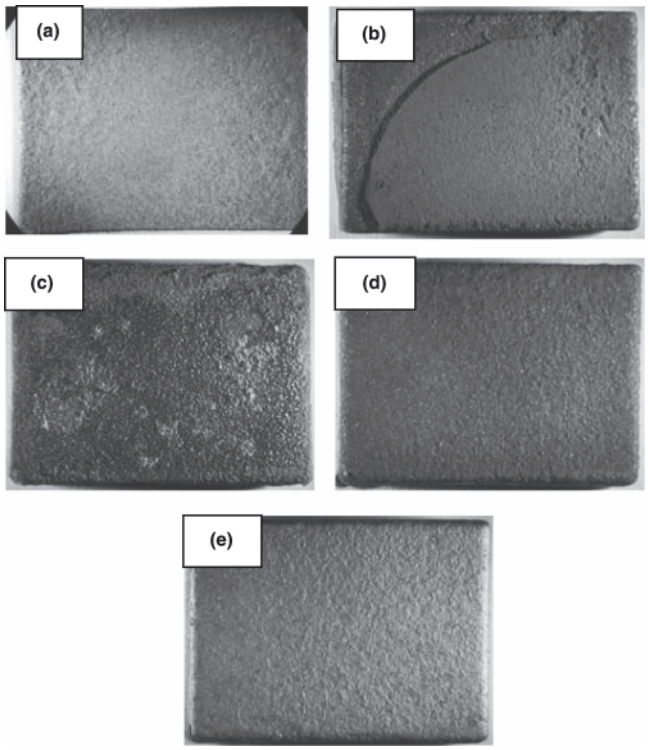

Fig. 3 Surface macrograph for the Superfer 800 H subjected to cyclic oxidation in air at 900 °C after 50 cycles: (a) uncoated; (b) Cr_3C_2-NiCr-coated; (c) NiCrBSi-coated; (d) Stellite-6-coated; and (e) Ni-20Cr-coated

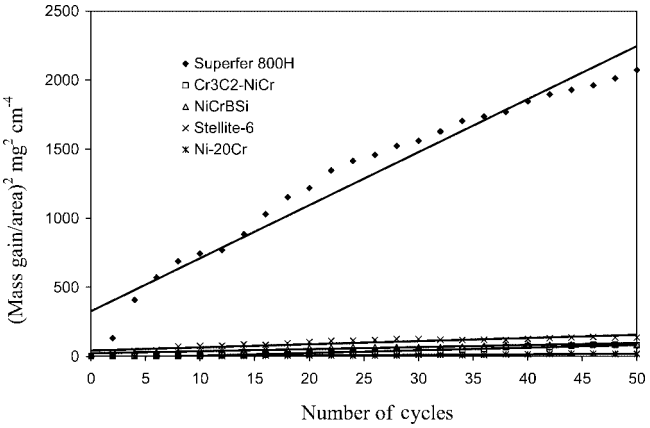

Fig. 4 The plot of the mass gain/area squared versus the number of cycles plot for coated and uncoated superalloy Superfer 800H specimens subjected to cyclic oxidation for 50 cycles in Na_2SO_4-60%V_2O_5 a t
900 °C

Table 1 Values of the parabolic rate constant K_p

Description	K_p 10^{-10} g^2 cm^{-4} s^{-1}
Uncoated superalloy	106.668
Ni-20Cr-coated	1.180
NiCrBSi-coated	4.131
Cr_3C_2-NiCr-coated	5.363
St-6-coated	6.308

Figure 4 shows the plot of the mass gain/area squared versus the number of cycles, and it can be inferred that the coated superalloys follow the parabolic law, which indicates that all of the coatings have shown a tendency to act like diffusion barriers to the corroding species. Table 1 shows the values of the parabolic rate constant K_p for the specimens studied.

3.2 Scanning Electron Microscopy/Energy-Dispersive X-Ray Analysis of the Scales

Micrographs obtained using a scanning electron microscope showing the surface morphology of the substrate and the coated superalloy specimens after cyclic hot corrosion at 900 °C are shown in Fig. 5. The cracks formed in the scale of the uncoated superalloy are clearly visible (Fig. 5a). The EDAX analysis for the uncoated specimen has shown Fe_2O_3 to be the predominant phase. The point analysis of Cr_3C_2-NiCr-coated specimen shows Cr_2O_3 as the principal phase along with a small percentage of the Fe_2O_3, MnO, and SiO_2 phases. The scale of the NiCrBSi-coated specimen was found to be rich in SiO_2, whereas the Ni-20Cr coating scale was found to be enriched with NiO. The EDAX analysis further identified CoO and Cr_2O_3 as the main phases, and small amounts of SiO_2, NiO, Fe_2O_3, and MnO were found in the scale of Stellite-6 coated superalloy.

3.3 X-Ray Diffraction Analysis

The XRD analysis was carried out with Bruker AXS D-8 Advance Diffractometer (Germany) with CuKα radiation. The diffraction patterns of the hot corroded specimens after 50 cycles have been shown in the Fig. 6. Various phases revealed by the XRD analysis are presented in Table 2.

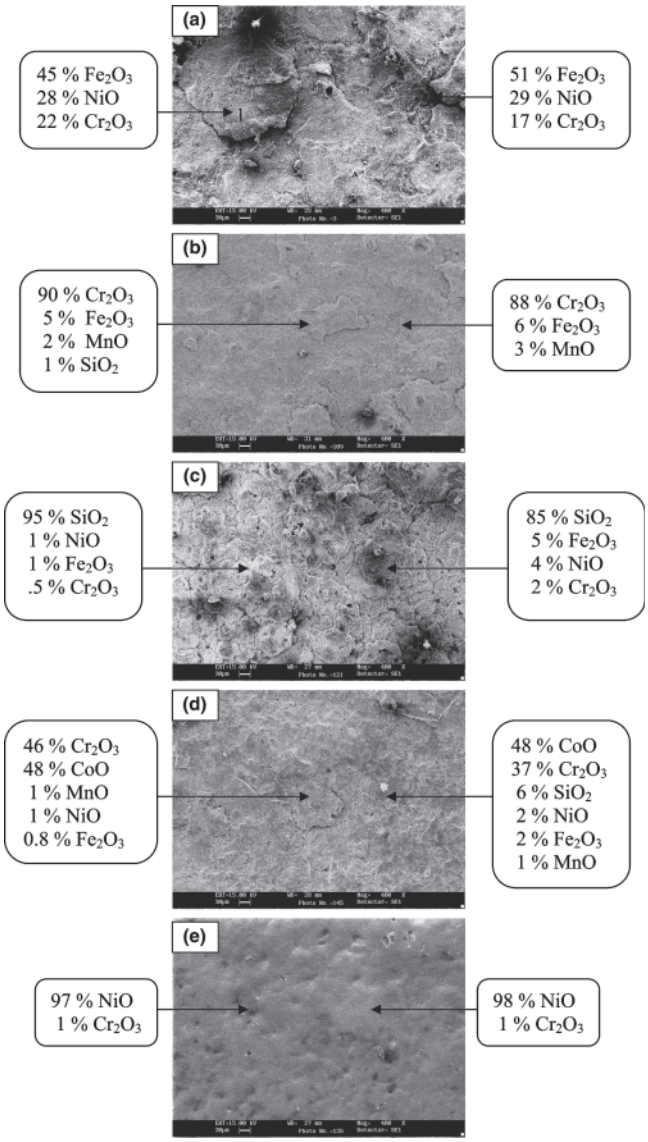

Fig. 5 Surface scale morphology and EDAX analysis for the Superfer 800H specimen subjected to cyclic oxidation in air at 900 °C at 400× magnification: (a) uncoated; (b) Cr_3C_2-NiCr-coated; (c) NiCrBSi-coated; (d) Stellite-6-coated; and (e) Ni-20Cr-coated

3.4 Cross Section Analysis of the Oxide Scale

Cross sections of the corroded samples were cut, mounted in transoptic mounting resin, and mirror-polished to obtain x-ray mapping of the different elements present across the scale.

Elemental x-ray mapping of the cross section of the Cr_3C_2-NiCr-coated superalloy that was subjected to cyclic oxidation at 900 °C in Na_2SO_4-60%V_2O_5 after 50 cycles (Fig. 7) indicated that the dense scale mainly consisted of chromium, with nickel also present in a scattered manner. Some pockets in the scale show depletion of chromium wherever nickel is present in a higher concentration. Aluminum, titanium, and manganese have shown their presence at the interface between the scale and the substrate in the form of prominent thin streaks. Some traces of iron could be seen in the topmost layer of the scale

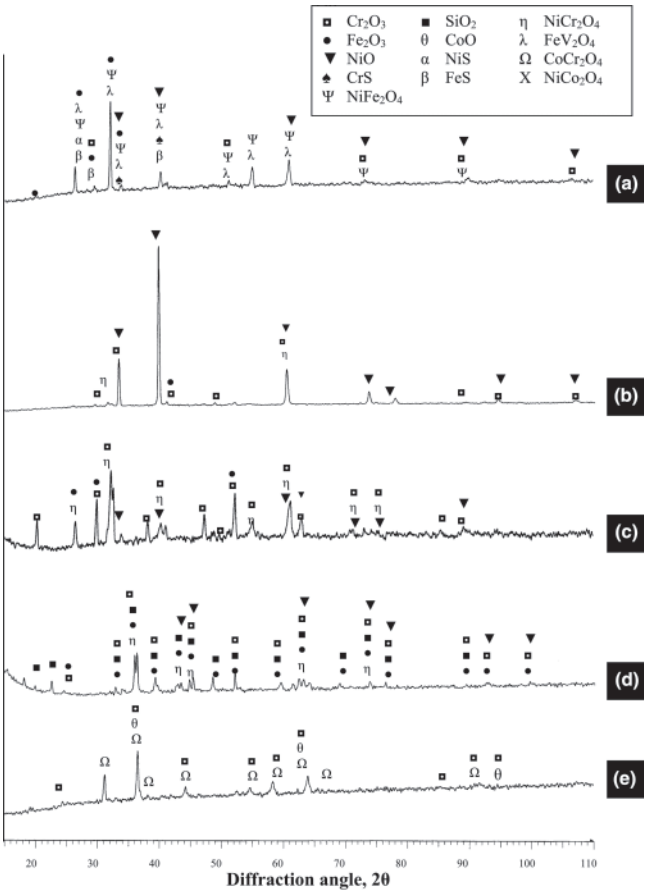

Fig. 6 The XRD patterns for the superalloy Superfer 800H subjected to cyclic oxidation in Na_2SO_4-60%V_2O_5 at 900 °C after 50 cycles: (a) uncoated; (b) Ni-20Cr-coated; (c) Cr_3C_2-NiCr-coated; (d) NiCrBSi-coated; and (e) Stellite-6-coated

Table 2 Major and minor phases identified by XRD analysis of the hot corroded specimens after 50 cycles

Description	Major phases	Minor phases
Uncoated superalloy	Fe_2O_3, NiO, $NiFe_2O_4$, Ni $(VO_3)_2$, NiS, CrS, and FeS	Cr_2O_3
Cr_3C_2-NiCr-coated superalloy	NiO, Cr_2O_3, $NiCr_2O_4$, and Fe_2O_3	…
NiCrBSi-coated superalloy	NiO, Cr_2O_3, $NiCr_2O_4$, Fe_2O_3, and SiO_2	…
Stellite-6-coated superalloy	CoO, Cr_2O_3, and $CoCr_2O_4$	…
Ni-20Cr-coated superalloy	NiO and Cr_2O_3	$NiCr_2O_4$

and in the scale just above the coating substrate interface, which indicate the diffusion of iron from the substrate to the scale. The diffusion of silicon has also been noticed throughout the scale from the base superalloy, and has also formed a thin streak at the scale-substrate interface. Vanadium and sulfur, which seems to have penetrated into the scale along the splat boundaries, were found to be present in trace amounts.

The EPMA analysis of the corroded Ni-20Cr-coated superalloy has been compiled in Fig. 8. The scale shows a lamellar structure, in which the topmost layer consists mainly of nickel. Iron has also diffused into this layer from the base alloy. Beneath this layer, the scale was found to be rich in nickel and chromium. A thick band of chromium was formed in the middle of the scale. The scale showed the depletion of nickel wherever chromium was present in higher concentration, and vice versa. Iron has also formed a thick band in the scale just above the interface between the base alloy and the scale. Nickel seems to have diffused from the coating into the substrate. The traces of sulfur, sodium, and vanadium were present throughout the scale, and these species seem to have migrated along the splat boundaries.

X-ray mapping of the NICrBSi-coated superalloys (Fig. 9) indicates a dense scale consisting mainly of nickel, silicon, and chromium. The topmost layer of the scale was found to be rich in silicon, with some traces of nickel, chromium, and iron. The presence of aluminum indicates its tendency to form clusters at the coating-substrate interface where all other elements are found to be depleted.

A similar analysis of Stellite-6-coated superalloys (Fig. 10) shows that the scale is mainly rich in chromium and cobalt along with some nickel. Some traces of iron are present throughout the scale, indicating its diffusion from the base alloy. Aluminum has shown its presence in the form of clusters, mainly at the coating-substrate interface, where all other elements are found to be depleted. The presence of vanadium has also been revealed in the scale, thereby indicating its ingress.

4. Discussion

The bare superalloy showed intense spalling as well as sputtering, and the mass gain was enormous. The mass gain graph (Fig. 1) shows that the mass increases continuously, although the rate of increase is high during the initial period of exposure. This rapid increase in mass gain is most likely due to the rapid diffusion of oxygen through the molten salt layer. In the temperature range of 900 °C, the Na_2SO_4 and 60%V_2O_5 will combine and form $NaVO_3$, having a melting point of 610 °C as proposed by Kolta et al. (Ref 34).

$$Na_2SO_4 + V_2O_5 = 2NaVO_3(l) + SO_2 + \tfrac{1}{2}O_2 \quad \text{(Ref 42)}$$

This $NaVO_3$ acts as a catalyst and also serves as an oxygen carrier to the base alloy, which will lead to the rapid oxidation of the basic elements of the superalloy to form the protective oxide scale. So, in the earlier stages of hot corrosion there is a rapid increase in the mass of the uncoated specimen. The rapid increase in mass gain during the initial hours was also reported by Tiwari and Prakash (Ref 35) and Singh et al. (Ref 31) in their studies on the hot corrosion behavior of the Fe-based superalloy. A slower increase in mass gain after the initial rise is probably due to the simultaneous growth and dissolution of oxide scale in the molten salt due to the reaction $Cr_2O_3 + 4NaVO_3 \rightarrow 2Na_2CrO_4 + V_2O_5 + O_2$ (Ref 36, 37). Fryburg et al. (Ref 38) have suggested that this Na_2CrO_4 evaporates as a gas.

Intensive spalling of the scale of the uncoated superalloy as observed can be attributed to the severe strain developed as a result of Fe_2O_3 precipitation from the liquid phase and the interdiffusion of intermediate layers of iron oxide, as reported by Sachs (Ref 39). Further, the presence of four different phases in a thin layer might have imposed severe strain on the film, which may result in the cracking and exfoliation of the

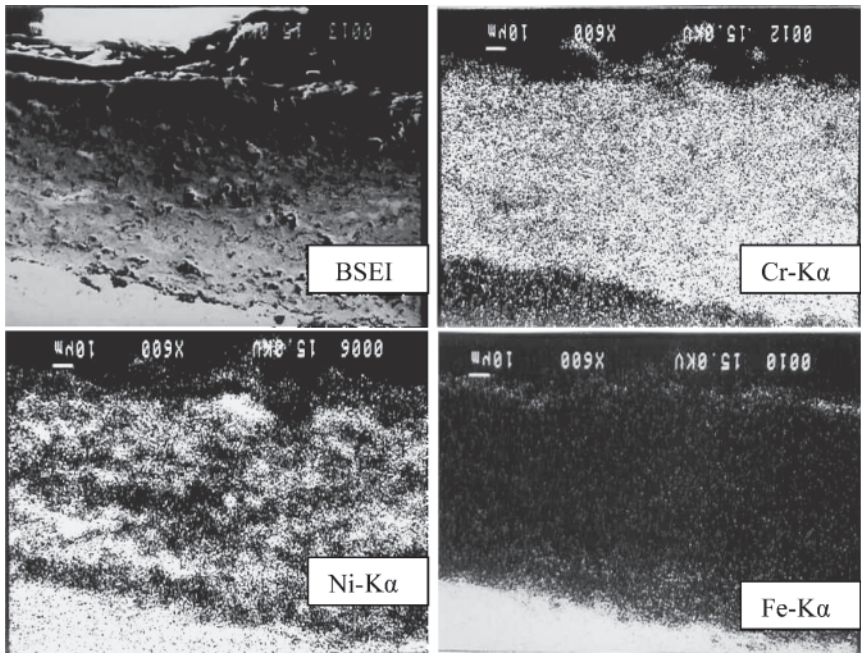

Fig. 7 Composition image backscattered electron image (BSEI) and x-ray mapping of the cross section of the Cr_3C_2-NiCr-coated superalloy subjected to cyclic oxidation at 900 °C in Na_2SO_4-60%V_2O_5 after 50 cycles

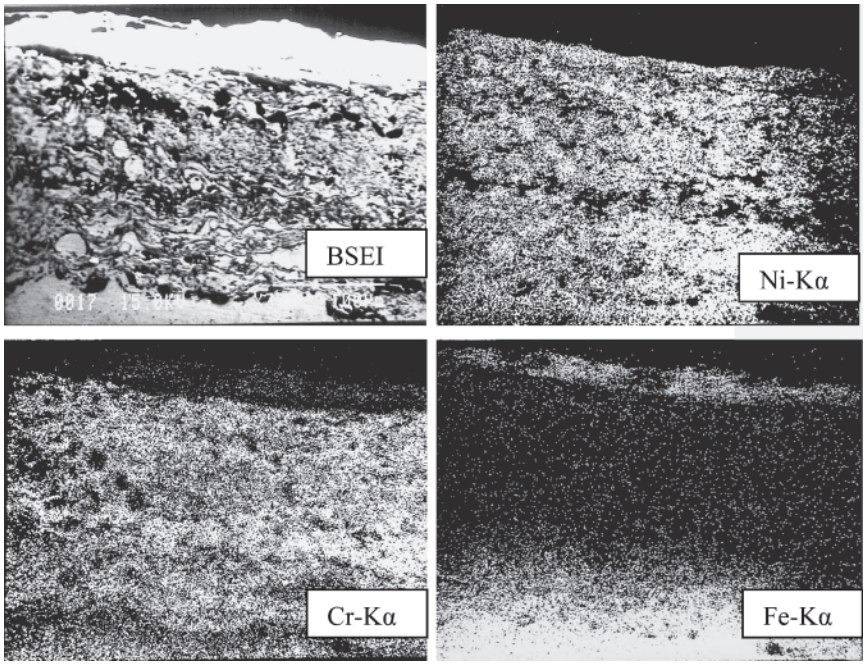

Fig. 8 Composition image BSEI and x-ray mapping of the cross section of the Ni-20Cr wire-coated superalloy subjected to cyclic oxidation at 900 °C in Na_2SO_4-60%V_2O_5 after 50 cycles

scale. The cracks may have allowed the aggressive liquid phase to reach the metal substrate (Ref 39).

Thermal cycles may lead to the spalling/peeling of the oxides formed on the surface of the coatings, especially on the edges of the specimens (Ref 33), which may be attributed to the different values of the thermal expansion coefficients of the coatings and the substrate, as reported by Singh et al. (Ref 31), Niranatlumpong et al. (Ref 40), and Sidhu (Ref 41). Niranatlumpong et al. (Ref 40) were of the opinion that the spallation could be initiated by the rapid growth of void-like defects lying adjacent to coating protuberances, at which point tensile radial stress developed during cooling as a result of the maximum thermal contraction mismatch between the oxide and the coating. The formation of cracks in the coating originates from stresses developed in the deposit or at the coating-base metal interface (Ref 42). Some elements, like Fe, might have diffused outward through these cracks to form their oxides or spinels, as has been revealed by XRD and EDAX analysis.

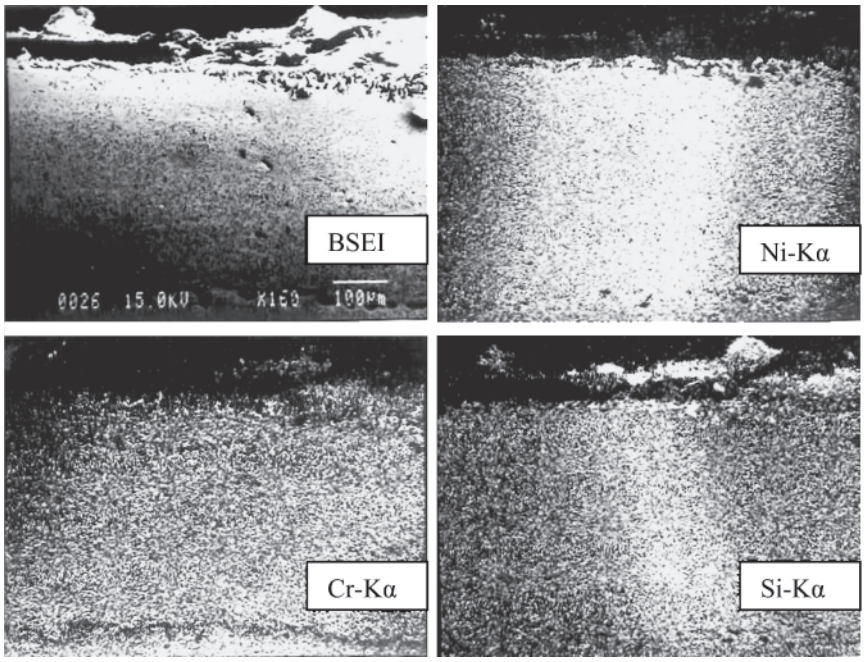

Fig. 9 Composition image BSEI and x-ray mapping of the cross section of the NiCrBSi-coated superalloy subjected to cyclic oxidation at 900 °C in Na_2SO_4-60%V_2O_5 after 50 cycles

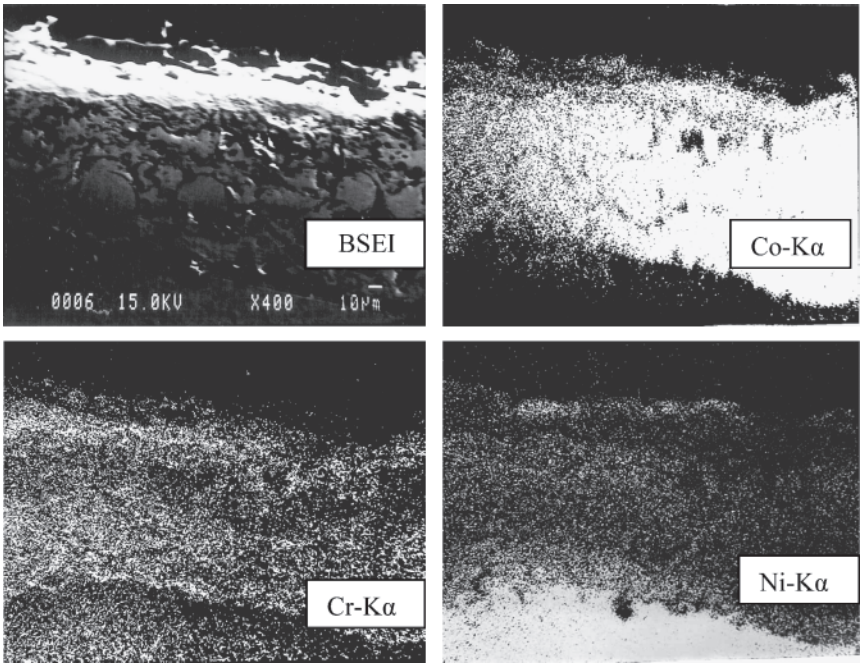

Fig. 10 Composition image BSEI and x-ray mapping of the cross section of the Stellite-6-coated superalloy subjected to cyclic oxidation at 900 °C in Na_2SO_4-60%V_2O_5 after 50 cycles

It can be inferred from Fig. 4 that all of the coatings on Superfer 800H superalloys followed the parabolic law, which indicates that the scales formed have shown the tendency to act as a diffusion barrier to corrosive species. This shows the corrosion protective behavior of the coatings.

The Ni-20Cr coating has shown high resistance to hot corrosion and has provided the best protection for the base alloy because it has been found to be successful in reducing the mass gain by 90%. This may be attributed to the presence of protective oxides of nickel and chromium, and a spinel of nickel and chromium, as indicated by the XRD and EDAX analysis. Singh et al. (Ref 31), Sidhu (Ref 41), Longa-Nava et al. (Ref 43), and Calvarin et al. (Ref 44) have reported almost similar findings. The formation of small amounts of Fe_2O_3, as indicated by EDAX/XRD analysis, may be due to the diffusion of iron from the substrate to the coating. The EPMA analysis also shows the diffusion of iron from the substrate to the coating and the diffusion of nickel from the coating to the substrate.

The diffusion of iron from the substrate to the coating and of nickel from the coating to the substrate was also noticed by Sundararajan et al. (Ref 45), Singh et al. (Ref 31), and Sidhu (Ref 41).

The corrosion resistance of Cr_3C_2-NiCr- and NiCrBSi-coated alloys could be due to the formation of phases like Cr_2O_3, NiO, and $NiCr_2O_4$. Additional protective phases of SiO_2 are responsible for the hot corrosion protective behavior of the NiCrBSi coating. The formation of small amounts of Fe_2O_3, as indicated by XRD/EDAX analysis, may be due to the diffusion of iron from the substrate, which was also noticed by Sundararajan et al. (Ref 45), Singh et al. (Ref 31), and Sidhu (Ref 41). The EPMA analysis of the Cr_2C_3-NiCr-coated superalloy reveals the diffusion of Si from the substrate to the coating, which was also observed by Singh (Ref 46). The Cr_3C_2-NiCr-coated alloy has shown slightly better corrosion resistance than the NiCrBSi-coated alloy, whereas the corrosion resistance of both coatings has been found to be less than that of the Ni-20Cr-coated alloy. However, they performed better than Stellite-6-coated alloy.

The Stellite-6 coating has shown the least resistance among the coatings studied. This may be attributed to the spalling of the coating as well as of the oxide scale. The protection shown by this coating may be due to the formation of oxides of chromium, and of spinels of chromium and cobalt. Luthra (Ref 47) proposed that the formation of spinels might stop the diffusion activities through the cobalt oxide (CoO), which in turn suppresses the further formation of this oxide. Luthra (Ref 47) further opined that increases in the growth of $CoCr_2O_4$ and Cr_2O_3 in competition with the formation of CoO and Co_3O_4 increases the corrosion resistance of alloys. The formation of the CoO, $CoCr_2O_4$, and Cr_2O_3 phases revealed by XRD and EDAX analysis is in accordance with the results of studies by Singh et al. (Ref 31), Sidhu (Ref 41), and Luthra (Ref 47).

5. Conclusions

The bare superalloy underwent intense spalling, sputtering, and peeling of the scale, and the mass gain was enormous in the molten salt environment of Na_2SO_4-60%V_2O_5 at 900 °C.

The HVOF-sprayed Ni-20Cr wire coatings and the Cr_3C_2-NiCr, NiCrBSi, and Stellite-6 powder coatings, when deposited with given parameters, are found to be very useful in developing hot corrosion resistance in a Fe-based superalloys, namely, Superfer 800H.

A Ni-20Cr wire coating has high corrosion resistance and provides the best protection to the base alloy. It has been found to be successful in reducing the mass gain by 90% of that gained by bare superalloys, which may be due to the presence of oxides of nickel and chromium and their spinels.

The hot corrosion resistance shown by the Cr_3C_2-NiCr coating is slightly better compared with the NiCrBSi coating, whereas the hot corrosion resistance of both the coatings has been found to be less than that of the Ni-20Cr coating. However, they performed better than the Stellite-6 coating. The Cr_3C_2-NiCr and NiCrBSi coatings have shown the formation of protective phases like Cr_2O_3, NiO, and $NiCr_2O_4$. In addition, the SiO_2 protective phase is formed in the NiCrBSi coating.

The Stellite-6 coating has shown, relatively, the lowest hot corrosion resistance among the coatings studied, which may be attributed to the spalling of the oxide scale as well as of the coating. The protection shown by this coating may be due to the formation of oxides of chromium and of spinels of chromium and cobalt.

There was marginal cracking/spalling observed in the case of the Stellite-6 coating during hot corrosion studies, whereas it was negligible in the case of the Ni-20Cr coating. This may be attributed to the different values of thermal expansion coefficients of the coatings and the substrate.

The spallation and peeling of the oxide scale was negligible in the NiCrBSi coating, as the addition of silicon and boron can promote the formation of continuous and dense scale in the initial corrosion stage and can improve the adherence of the outer scale to the coating in the subsequent hot corrosion process.

References

1. P. Hancock, Vanadic and Chloride Attack of Superalloys, *Mater. Sci. Technol.,* 1987, 3, p 536-544
2. N. Eliaz, G. Shemesh, and R.M. Latanision, Hot Corrosion in Gas Turbine Components, *Eng. Failure Anal.,* 2002, 9, p 31-43
3. N.S. Bornstein, M.A. Decrescente, and H.A. Roth, The Relationship Between Relative Oxide Ion Content of Na_2SO_4, the Presence of Liquid Metal Oxides and Sulfidation Attack, *Metall. Trans.,* 1973, 4, p 1799-1810
4. G.H. Meier and F.S. Pettiit, "Corrosion of Superalloy," Conference on High Temperature (London, U.K.), The Institute of Metals, February 1986
5. J.A. Goebel, F.S. Pettit, and G.W. Coward, Mechanisms for the Hot Corrosion of Nickel-Base Alloys, *Met. Trans.,* 1973, 4, p 261-275
6. T.S. Sidhu, R.D. Agrawal, and S. Prakash, Hot Corrosion of Some Superalloys and Role of High-Velocity Oxy-Fuel Spray Coatings: A Review, *Surf. Coat. Technol.,* 2005, 198, p 441-446
7. P.S. Sidky and M.G. Hocking, Review of Inorganic Coatings and Coating Processes for Reducing Wear and Corrosion, *Br. Corrosion J.,* 1999, 34 (3), p 171-183
8. J.R. Nicholls and D.J Stephenson, High Temperature Coatings for Gas Turbines, *Surf. Eng.,* 1991, 22, p 156-163
9. R. Mevrel, State of the Art on High-Temperature Corrosion-Resistant Coatings, *Mater. Sci. Eng. A,* 1989, 120, p 13-24
10. Th.F. Weber, High-Velocity Oxy-Fuel Spraying, *Mater. Sci. Forum,* 1994, 163, p 573-578
11. G. Iron, U. Zanchuk, and C.C. Berndt, Comparison of MCrAlY Coatings Sprayed by HVOF and Low Pressure Processes, Thermal Spray Coatings: Research, Design and Aplications, C.C. Berndt and T.F. Bernecki, Ed., June 7-11, 1993 (Anaheim, CA), ASM International, 1993, p 191-197
12. I. Gurappa, Influence of Alloying Elements on Hot Corrosion of Superalloys and Coatings: Necessity of smart Coatings for Gas Turbine Engines, *Mater. Sci. Technol.,* 2003, 19, p 178-183
13. M.G. Hocking, Coatings Resistant to Erosive/Corrosive and Severe Environments, *Surf. Coat. Technol.,* 1993, 62, p 460-466
14. I. Gurrappa, Identification of Hot Corrosion Resistant MCrAlY Based Bond Coatings for Gas Turbine Engine Applications, *Surf. Coat. Technol.,* 2001, 139, p 272-283
15. M. Rosso and A. Bennani, "Studies of New Applications of Ni-Based Powders for Hardfacing Processes," Paper presented at PM World Congress Thermal Spraying/Spray Forming, Granada, Spain, October, 1998, p 524-530
16. R. Knight and R.W. Smith, HVOF Sprayed 80/20 NiCr Coatings–Process Influence Trends, *Thermal Spray: International Advances in Coatings Technology,* C.C. Berndt, Ed., May 25-June 5, 1992 (Orlando, FL), ASM International, 1992, p 159
17. M.R. Dorfman and J.A. DeBarro, *Thermal Spraying: Current Status and Future Trends,* Akira Ohmori, Ed., May 22-26, 1995 (Kobe, Japan), High Temperature Society of Japan, 1995, p 567
18. M.D.F. Harvey, A.J. Sturgeon, F.J. Blunt, and S.B. Dunkerton, *Thermal Spraying: Current Status and Future Trends,* Akira Ohmori, Ed., May 22-26, 1995 (Kobe, Japan), High Temperature Society of Japan, 1995, p 531-535
19. B. Nordmand, H. Liao, O. Landemarre, C. Coddet, and J. Pagetti, *Thermal Spray: Meeting the Challenges of the 21st Century,* C. Coddet, Ed., May 25-29, 1998 (Nice, France), ASM International, 1998, p 69
20. H. Edris, D.G. McCartney, and A.J. Sturgeon, Microstructural Char-

acterization of High Velocity Oxy-Fuel Sprayed Coatings of Inconel 625, *J. Mater. Sci.,* 1997, 32, p 863
21. F. Otsubo, H. Era, and K. Kishitake, Structure and Phases in Nickel-Base Self-Fluxing Alloy Coating Containing High Chromium and Boron, *J. Thermal Spray Technol.,* 2000, 91, p 107-113
22. S. Lebaili, S. Hamar, and S. Thibault, Equilibres Liquide-Solide Dans Le Systemr Ni-B-Si Dans la Region Riche en Nickle, *Acta Metall.,* 1987, 35 (3), p 701-710, in French
23. Y. Kawahara, Development and Application of High Temperature Corrosion-Resistant Materials and Coatings for Advanced Waste-to-Energy Plants, *Mater. High Temp.,* 1997, 14 (3), p 261-268
24. E.J. Morgan-Warren, Thermal Spraying for Boiler Tube Protection, *Weld. Met. Fabric.* (Jan./Feb.), 1992, p 25-31
25. K.C. Antony, Wear-Resistant Cobalt-Base Alloys, *J Met.,* 1983, 39, p 52
26. P. Crook, *Properties and Selection: Non-Ferrous Alloys and Special-Purpose Materials,* Vol 10, *ASM Handbook,* 2nd ed., ASM International, 1993, p 446
27. D. Zhang, S.J. Harris, and D.G. McCartney, *International Thermal Spray Conference,* E. Lugscheider and C.C. Berndt, Ed., March 4-6, 2002 Essen, Germany), DVS Deutscher Verband für Schweissen, 2002, p 500-505
28. S.N. Tiwari, "Investigations on Hot Corrosion of Some Fe-, Ni- and Co-Base Superalloy in Na_2SO_4-V_2O_5 Environment Under Cyclic Conditions," Ph.D. dissertation, Indian Institute of Technology Roorkee, Utranchal, India, 1997
29. A. Ul-Hamid, Diverse Scaling Behavior of the Ni-20Cr Alloy, *Mater. Chem. Phys.,* Vol 80, 2003, p 135-142
30. B.S. Sidhu and S. Prakash, Evaluation of the Corrosion Behaviour of Plasma-Sprayed Ni3Al Coatings on Steel in Oxidation and Molten Salt Environments at 900 °C, *Surf. Coat. Technol.,* 2003, 166, p 89-100
31. H. Singh, D. Puri, and S. Prakash, Some Studies on Hot Corrosion Performance of Plasma Sprayed Coatings on a Fe-Based Superalloy, *Surf. Coat. Technol.,* 2005, 192, p 27-38
32. S.E. Sadique, A. H. Mollah, M.S. Islam, M.M. Ali, M.H.H. Megat, and S. Basri, High-Temperature Oxidation Behavior of Iron-Chromium-Aluminum Alloys, *Oxid. Met.,* 2000, 54 (5-6), p 385-400
33. Q.M. Wang, Y.N. Wu, P.L. Ke, H.T. Cao, J. Gong, C. Sun, and L.S. Wen, Hot Corrosion Behaviour of AIP NiCoCrAlY(siB) Coatings on Nickel Base Superalloys, *Surf. Coat. Technol.,* 2004, 186 (3), p 389-397
34. G.A. Kolta, I.F. Hewaidy, and N.S. Felix, Reactions Between Sodium Sulphate and Vanadium Pentoxide, *Thermochim. Acta,* 1972, 4, p 151-164
35. S.N. Tiwari and S. Prakash, "Studies on the Hot Corrosion Behaviour of Some Superalloys in Na_2SO_4-V_2O_5," Paper presented at Symposium on Localised Corrosion and Environmental Cracking (SOLCEC) (Kalpakkam, India), 1997, C-33
36. M. Seiersten and P. Kofstad, The Effect of SO_3 on Vanadate-Induced Hot Corrosion, *High Temp. Technol.,* 1987, 3 (5), p 115-122
37. J. Swaminathan, S. Raghavan, and S.R. Lyer, Studies on the Hot Corrosion of Some Nickel-Base Superalloys by Vanadium Pentoxide, *Trans. Indian Inst. Metals,* 1993, 3, p 175-181
38. G.C. Fryburg, F.J. Kohl, and C.A. Stearns, Chemical Reactions Involved in the Initiation of Hot Corrosion of IN-738, *J. Electrochem. Soc.,* 1984, 131 (12), p 2985-2996
39. K. Sachs, Accelerated High Temperature Oxidation due to Vanadium Pentoxide, *Metallurgia,* April, 1958, p 167-173
40. P. Niranatlumpong, C.B. Ponton, and H.E. Evans, The Failure of Protective Oxides on Plasma-Sprayed NiCrAlY Overlay Coatings, *Oxid. Met.,* 2000, 53 (3-4), p 241-258
41. B.S. Sidhu, "Studies on the Role of Coatings in Improving Resistance to Hot Corrosion and Degradation," Ph.D. dissertation, Indian Institute of Technology Roorkee, Utranchal, India, 2003
42. G.R. Heath, P. Heimgartner, G. Irons, R. Miller, and S. Gustafsson, An Assessment of Thermal Spray Coating Technologies for High Temperature Corrosion Protection, *Mater. Sci. Forum,* 1997, 251-254, p 809-816
43. Y. Longa-Nava, Y.S. Yang, M. Takemoto, and R.A. Rapp, Hot Corrosion of Nickel-Chromium and Nickel-Chromium-Aluminum Thermal-Spray Coatings by Sodium Sulfate-Sodium Metavanadate Salt, *Corrosion,* 1996, 52 (9), p 680-689
44. G. Calvarin, R. Molins, and A.M. Huntz, Oxidation Mechanism of Ni-20Cr Foils and Its Relation to the Oxide-Scale Mircrostructure, *Oxid. Met.,* 2000, 53 (1-2), p 25-48
45. S. Sundararajan, S. Kuroda, K. Nishida, T. Itagaki, and F. Abe, Behaviour of Mn and Si in the Spray Powders During Steam Oxidation of Ni-Cr Thermal Spray Coatings, *ISIJ Int.,* 2004, 44, p 139-144
46. H. Singh, "Hot Corrosion Studies on Plasma Spray Coatings over Some Ni- and Fe-Based Superalloys," Ph.D. dissertation, Indian Institute of Technology Roorkee, Utranchal, India, 2005
47. K.L. Luthra, Kinetics of the Low Temperature Hot Corrosion of Co-Cr-Al Alloys, *J. Electrochem. Soc.,* 1985, 132 (6), p 1293-1298